Shallow Geophysical Constraints on Displacement and Segmentation of the Pahrump Valley Fault Zone, California-Nevada Border

John Louie, Gordon Shields, Gene Ichinose, Michael Hasting, Gabriel Plank, and Steve Bowman

Seismological Lab (174), University of Nevada, Reno, NV 89557-0141
(702) 784-4219; fax (702) 784-1833; louie@seismo.unr.edu

Submitted to
Proceedings of the Basin and Range Province Seismic Hazards Summit
May 12-15, 1997
Reno, Nevada

For publication by the Utah Geological Survey, Cedar City, Utah.

TABLE OF CONTENTS

ABSTRACT

The Pahrump Valley fault zone (PVFZ) is active and represents a potential seismic hazard for Las Vegas. Combining as many as six segments over a total length of more than 100 km, the PVFZ may be able to produce a magnitude 7 event only 50 km from the metropolitan area. We employ the seismic reflection, gravity, magnetic, and electromagnetic geophysical techniques to locate segments of the PVFZ and examine their subsurface geometry. Geophysical techniques can provide clues to segmentation and rates of activity in advance of detailed trench studies, and can uncover deeper and older displacements. On the PVFZ segment in southern Pahrump Valley we can locate fault strands near three Holocene scarps from pronounced magnetic and soil conductivity anomalies. We also observe truncations and limit the vertical offsets of reflective ash beds in shallow seismic profiles across two of these scarps. The sharpness of the magnetic and soil conductivity anomalies appears to correlate with the relative geomorphic youth of the scarps. These three geophysical techniques in combination can locate faults that lack clear surface expressions. A similar study of PVFZ strands in southern Stewart Valley shows clear evidence for more than 18 m of Holocene dextral displacement in a 3-d seismic survey, but without any vertical component of displacement. The Pahrump Valley fault zone appears to have little evidence for segmentation that could limit earthquake rupture length to less than 60 km anywhere in Pahrump Valley. The 18 m minimum displacement of Wisconsin and pre-Wisconsin age lacustrine formations likely results from a Holocene dextral slip rate above 0.1 mm/yr; the rate is certainly larger than 0.03 mm/yr, and probably less than 2 mm/yr.

PAHRUMP VALLEY FAULT ZONE

Although hidden on many maps by its location usually within 1 km of the California-Nevada state line, the Pahrump Valley fault zone (PVFZ) is the longest seismogenic structure within 100 km of the Las Vegas metropolitan area (fig. 1). Only 50 km distant at its closest reach, it extends at least 60 km from Stewart Valley to southern Pahrump Valley (Hoffard, 1991), equal in length to any one of the four segments of the Death Valley fault system proposed by Sawyer et al. (1996). Additional segments of the PVFZ may well extend north of Stewart Valley into Ash Meadows and Amargosa Valley as proposed by Donovan (1991) and Schweickert and Lahren (1994). To the south, it extends through Mesquite Valley (MIT Field Geophys. Course, 1985) and possibly into Sandy and even Ivanpah Valleys (Burt Slemmons, pers. comm. 1997). Thus possible rupture lengths range from 60 to 150 km, implying the potential for events with M_W magnitudes between 6.9 and 7.2. Such an event on the PVFZ could produce rock-site accelerations in the Las Vegas metropolitan area of up to 20% g, and possibly larger spectral accelerations at frequencies of two hertz or below (Su and Anderson, 1996).

Given the 12 mm/yr of the 56 mm/yr of Pacific-North America plate motion that diverts into the Eastern Mojave shear zone (Dokka and Travis, 1990) and the Walker Lane, Slemmons (1996) accounts for 2 mm/yr on the Owens Valley fault system, 2 mm/yr in Panamint Valley, and now 4 mm/yr on the Death Valley fault system (Sawyer et al., 1996). This leaves 4 mm/yr for all Basin and Range motions east of Death Valley. Structures such as the Eglington scarp and the Frenchman Mountain fault in Las Vegas Valley show inconclusive evidence of rates as high as 1 mm/yr. However, the PVFZ may be the only candidate for a structure east of Death Valley long enough to show a rate as high as 1 mm/yr.

dePolo and Ramelli (1996) find rates in southern Nevada to average near 0.01 mm/yr, largely a result of the concentration of neotectonic studies around Yucca Mountain, an order of magnitude below the 0.1 mm/yr average deformation rates for Great Basin faults. Seismicity rates presented by Smith et al. (1996) support such lower rates in southern Nevada; except in association with Lake Mead reservoir induced seismicity, activity associated with the 1992 Little Skull Mountain and Rock Valley sequences, and a cluster of seismicity in southern Pahrump Valley. Anderson et al. (1995) examined a segment of the PVFZ that extends from the main segment in southern Pahrump Valley on a more northerly path past the west side of the Spring Mountains, perhaps following Nevada Highway 160 as far as U.S. Highway 95 (fig. 1). They measured scarp profiles in alluvium to estimate that two large M_w=7 had occurred in approximately the past 128 ka. They did not find any Holocene scarps on that segment, however.

We will examine the main segments of the PVFZ at two locations, in Southern Pahrump Valley at the Old Spanish Trail Highway, and in Stewart Valley near California Highway 178 and Nevada Highway 372 (fig. 1). Each of these localities crosses a section of the PVFZ that appears to differ from the other in its apparent style of faulting, and type of scarp exposure. The authors all contributed to a University of Nevada, Reno (UNR) course in Geophysical Applications that performs field exercises in the area every two years. Our objective is to investigate how inexpensive shallow geophysical exploration methods may allow some characterization of fault displacement amounts and styles on these two parts of the PVFZ, and describe localities most appropriate for more detailed paleoseismic investigations.

SOUTHERN PAHRUMP VALLEY

In southern Pahrump Valley, the PVFZ divides into three fault-line scarps, each dissected by headward erosion of the uplifted playa and alluvial surfaces (Hoffard, 1991). The scarp closest to the California-Nevada state line, which appears geomorphically youngest and sharpest, with about 10 m of relief, we call scarp 1. The scarps further from the state line, scarps 2 and 3, while about twice as high, have gentler slopes and appear more eroded (fig. 2). Piety (1996) presents a map suggesting scarp 1 may belong to themain fault segment that continues 60 km northwestward to Stewart Valley. Scarps 2 and 3 may instead be related to the more northerly-striking zone skirting the west side of the Spring Mountains examined by Anderson et al. (1995).

Shields et al. (1996) discuss the collection of geophysical profiles across the scarps (fig. 2), and establish the repeatability of both the conductivity and magnetic measurements, including the fact that the strike of the anomaly at scarp 1 follows the strike of the scarp. Note on fig. 2 that both types of anomaly suggest that all three scarps are fault-line scarps, with the topographic scarps having eroded back between 50 and 300 m from the fault break locations suggested by the anomalies.

At scarp 1 a tephra bed has been exposed by headward erosion, appearing to slump about a meter into the fault zone. We have not yet identified this tephra, nor its age. Based on work by Morrison (1991) and Hillhouse (1987) in the Tecopa and Chicago Valleys immediately to the west of Pahrump Valley, active lacustrine deposition ended no earlier than 0.16 Ma, with prominent tephras deposited at 0.76 Ma (Bishop), 0.9 Ma, and 2.01 Ma (Huckleberry Ridge). The Pluvial lake in Pahrump Valley drained north to or was contiguous with a lake in Stewart Valley, which drained north in turn to Ash Meadows and the Amargosa River; and so was at least occasionally tributary to Pluvial Tecopa Lake.

Despite the evidence at scarp 1 for vertical offset of tephra layers and other lacustrine beds, our attempts to model the magnetic anomaly at the scarp with a vertical fault displacement of a magnetic layer (fig. 3, lower) were not successful. Given the orientation of our survey with respect to Earth's magnetic field, the displacement anomaly cannot match the symmetry of the magnetic high in the data. A model placing a magnetic body as an inclusion within the steeply-dipping fault plane (fig. 3, upper) fits the symmetry better.

Shields et al. (1996) propose that Pluvial spring activity (as discussed by Quade et al., 1995) produced mineralization of the fault plane allowing the conductivity and magnetic observations. Under this mineralization hypothesis, scarp 1 appears to have the most recent motion and best preserved mineralization, with the largest anomalies, while scarps 2 and 3 appear to be associated with older and more degraded fault mineralization.

In addition to the shallow conductivity and magnetic measurements, we conducted more deeply-penetrating transient electromagnetic (TEM) soundings. Analysis of the three TEM soundings (fig. 4) shows distinct high-conductivity layers at about 10 m depth away from the fault zone, with only evidence of a very shallow conductivity high at scarp 1. The TEM soundings average over the 40 m^2 area of the transmitter loops above 20 m depths, and over larger areas at deeper depths. The sounding 200 m northeast of scarp 1 shows the apparently conductive tephra layer at the same absolute elevation as the layer exposed at scarp 1, since the ground surface at the sounding to the northeast is about 10 m higher in elevation than the surface at the scarp 1 sounding (fig. 4). The surface elevation at the sounding 200 m southwest of scarp 1 is at about the same elevation as the scarp 1 sounding. The exposed, conductive tephra at the scarp agrees well with the coincident shallow ground conductivity high shown in fig. 2. The TEM technique and the time-domain depth inversion we use is not, however, expected to be sensitive to any layers below the uppermost conductive layer.

Two-dimensional seismic reflection profiles confirmed the lack of absolute vertical offset of the lake beds and tephra layers by the PVFZ at scarp 1 (fig. 5, upper). The reflection at 40 ms two-way travel time in the unmigrated section at left shows an approximately constant subsurface elevation after correction for surface elevation statics, with some slumping and disruption within a 70 m wide zone on the southwest edge of the surface fault-line scarp. The slumping may be part of a negative flower structure along an almost purely strike-slip PVFZ at scarp 1, or it may originate as a fault-trace graben due to a small extensional component of fault motion. This reflective bed thus cannot be the tephra layer exposed at scarp 1 and buried at 10 m away from the scarp; it is likely to be an older tephra buried about 20 m deeper.

The seismic section at scarp 2 (fig. 5, lower) also suggests a slumped tephra layer at about 60 m depth, more centered on the topographic scarp, with at least twice the vertical displacement. The image cannot rule out an absolute offset of the tephra layer of 40 m at scarp 2, and may instead suggest that scarp 2, and by inference scarp 3, have a much higher proportion of normal slip than does scarp 1. If scarps 2 and 3 belong to the north-trending segment of the PVFZ that defines the western edge of the Spring Mountains, then a larger proportion of dip-slip would not be surprising.

The geophysical investigations in southern Pahrump Valley suggest the PVFZ has its most recent, and almost purely strike-slip, motion at scarp 1, closest to the California-Nevada border. The other two scarps show older motions, possibly with larger proportions of dip slip.

STEWART VALLEY

Low-sun-angle aerial photography shows the PVFZ as a series of continuous scarps that follow within 1 km of the state line from southern Pahrump Valley to the southern end of Stewart Valley, directly west of the town of Pahrump (Hoffard, 1991). The highway running across the middle of fig. 6 is California 178/Nevada 372, and Ash Meadows Road extends to the north along the east side of the PVFZ. The intersecting east-west road is part of a residential development, and has been paved since the photo was taken about 1987. Several homes are now occupied within the development.

As the PVFZ enters southern Stewart Valley it turns to a more northerly strike, and may become the basin-bounding fault between Stewart Valley and the Montgomery Mountains to the east. Landowners along the PVFZ in central Stewart Valley report the water table at 9 or 10 m depth, and the fault is marked there by groves of tamarisk and other phreatophytes. The main trace of the PVFZ in southern Stewart Valley is visible near the left edge of fig. 6 as a continuous vegetation lineament. Additional traces to the right follow a series of spring mounds (Quade et al., 1995), or possibly terraces in the lake beds cut by wave action in the Pluvial lake. We targeted our work in Stewart Valley to a relatively simple stretch of the fault at the northward bend, between more complex sets of traces to the north and south. This location appears about midway along the fault trace between the highway and the development road (fig. 6).

Although the surface at this locality (fig. 7) exposes Pluvial lacustrine sediments and/or spring deposits, it is covered with a desert pavement of volcanic float washed from the hills to the east. The volcanic cobbles and rubble rendered no useful magnetic signal from the fault scarps at this locality; the rapidly varying field from surface float blocks swamped any anomalies from subsurface structures.

The gravity results of fig. 8 (top, triangles) can match a synthetic model (fig. 8, top, solid line) putting a small, approximately 50 m deep basin or shelf between the air-photo lineaments we call fault 1 and fault 2 (fig. 7). These possible fault locations are noted on the topographic profiles (fig. 8, bottom; fig. 9, top). As in southern Pahrump Valley, the EM-31 shallow conductivity measurements (fig. 8, center) produced clear anomalies centered on the surface lineaments and continuous along their strike. However, anomalies also appear that we have not been able to associate with any fault break on the ground or in the low-sun-angle aerial photography.

Unlike in southern Pahrump Valley, TEM surveys in Stewart Valley (fig. 9) did not identify discrete conductive layers, possibly because of the relatively shallow water table. Combining the eight TEM soundings into the pseudosection of fig. 9 (bottom), fault 1 appears to mark the edge of conductive lacustrine sediment filling the basin to the west. At fault 2 a low-conductivity anomaly near the surface suggests abundant silica cementation within the spring mound. The apparent very high conductivity below may be an artifact of the low-conductivity anomaly. The EM-31 shallow conductivity measurements only cover the very top layers of the pseudosection, and there does appear to be some correspondence between higher conductivities in the TEM results (fig. 9) and in the EM-31 profiles (fig. 8) at fault 1.

Ultra high-resolution three-dimensional seismic reflection surveying we carried out across fault 1 in Stewart Valley reveals the details of fault geometry and displacement. We laid out 11 lines across the fault (fig. 7) spaced at 3.05 m (10 ft), and recorded each line individually. Each line consisted of 48 fixed 100 Hz single-phone receivers, buried about 20 cm and tamped with soil. A source consisting of a 5 kg (12 lb) sledgehammer was hit against a 30 cm square 2 cm thick steel plate, set on the surface at each receiver point on each line. The 10 hits at each point were stacked by a Bison Galileo-21 seismic recorder, generously donated to the UNR Mackay School of Mines by the W. M. Keck Foundation.

Data reduction consisted of minimal bandpass filtering followed by true three-dimensional imaging using an interval velocity profile derived from analysis of a suite of constant-velocity stacked sections. The 3-d prestack depth imaging technique is almost identical to the Kirchhoff-sum migration of Louie et al. (1988), with operator aliasing controls as described by Lumley et al. (1994), but using boxcar instead of triangle antialias filters.

The front face of the image volume (fig. 10) shows interruptions in flat reflectors between 24 and 48 m depth that locate the subsurface fault break with a near-vertical dip, surfacing at the center of the volume (fig. 10, PVF). The upward curving of deeper reflectors near the sides of the volume is an artifact of low fold coverage near the ends of the survey lines. No measurable vertical offset of any of the layers is apparent, limiting the dip slip of PVFZ fault 1 in Stewart Valley to less than one meter. The depth slice at 48 m (fig. 10, right) shows the interruption of a layer by the fault trace at that depth, without vertical displacement.

The depth slice at 24 m (fig. 10, center) shows a lateral discontinuity on the northeast side of fault 1 that could arise at a fluvial channel wall, a facies change, or the side of a spring mound structure. The layer on the southwest side of the PVFZ fault 1 shows no similar lateral discontinuity within the image volume, proving that the discontinuity was dextrally displaced a minimum of 18 m into the image volume by PVFZ fault motion.

The image in fig. 10 establishes a minimum fault displacement on a sedimentary structure of unknown age. This structure, at 24 m depth, is likely much older than the most recent rupture, which fig. 7 shows as breaking the surface. Quade et al. (1995) establish a pre-Wisconsin Rancholabrean age range of 10 ka to less than 450 ka for spring mounds in Stewart and Pahrump Valleys.

Since the Pluvial lake in Stewart Valley served as an outlet for all discharge from the western Spring Mountains certainly as late as the Wisconsin Pluvial period, near-surface lacustrine deposits in Stewart Valley could be as young as 5-10 ka. The lateral offset at 24 m depth may well represent fault displacement of the top of a pre-Wisconsin age spring mound, within Wisconsin-age lake deposits.

Thus the 18 m minimum offset could represent a cumulative displacement rate as high as 1.8 mm/yr, if the spring mound has the 10 ka minimum age. Spring activity may have peaked earlier in southern Nevada, at 100-150 ka, suggesting that the displacement rate is likely above 0.1 mm/yr, about average for faults in the Great Basin (dePolo et al., 1996). Putting the spring mound at the earliest possible Rancholabrean age, we see that the Quaternary displacement rate on the PVFZ cannot be less than 0.03 mm/yr, well above the rate for smaller faults in southern Nevada.

CONCLUSIONS

Geophysical surveys across two sections of a major right-lateral strike-slip fault zone on the California-southern Nevada border have established that the Pahrump Valley Fault Zone maintains an almost completely strike-slip character from southern Pahrump Valley to southern Stewart Valley. Despite apparent changes in tectonic setting that suggested segmentation, the PVFZ is straight, continuous, purely strike-slip, and shows Holocene activity over a distance of more than 60 km. While this length of the fault may be a segment of a longer system possibly extending south into Mesquite Valley and north into Ash Meadows, segmentation hypotheses would propose that the main 60 km length in Pahrump Valley could rupture completely, producing an earthquake having a moment magnitude M_W as large as 7.2. Contrary to current assessments of regional seismic hazards to the Las Vegas metropolitan area, the 18 m minimum Holocene dextral displacement found by high-resolution 3-d seismic surveying in

Stewart Valley (fig. 10) establishes a displacement rate much greater than the average for faults in southern Nevada. The PVFZ may have a displacement rate above the 0.1 mm/yr average for faults in the Great Basin overall. As little as 50 km from the metropolitan area, the Pahrump Valley Fault Zone could pose the most significant seismic hazard to Las Vegas after the very active 4 mm/yr Death Valley fault system.

ACKNOWLEDGMENTS

This research was generously supported by the National Science Foundation under grant EAR-9405534, by the S. F. Hunt Fund of the UNR Mackay School of Mines, and by the W. M. Keck Foundation. Electromagnetic instruments were provided by Dr. Ken Taylor of the Desert Research Institute, and by Chet Lide of Zonge Geoscience Inc. The authors thank Chet Lide and D. Burt Slemmons for helpful reviews of the manuscript; and acknowledge the kind assistance of the California Dept. of Transportation, Inyo County, the Nevada Dept. of Transportation, Clark County, and Nye County. Students participating in the 1994 and 1996 field exercises were David Aglietti, Kip Allander, Steve Bowman, Russell Brigham, Ryan Crosbie, Michael Hasting, Andrew Hessel, Gene Ichinose, Zakir Kanbur, Sheander Ni, Jim Ollerton, Gordon Shields, Mike Sleeman, Lorenzo Trimble, Richard Tucker, and Hongbin Zhan.

An electronic version of this document is available at the location: http://www.seismo.unr.edu/ftp/pub/louie/talks/lvsh/gbshs.html

REFERENCES

Anderson, R. Ernest, Bucknam, Robert C., Crone, Anthony J., Haller, Kathleen M., Machette, Michael N., Personius, Stephen F., Barnhard, Theodore P., Cecil, Meridee J., Dart, Richard L., 1996, Characterization of Quaternary and suspected Quaternary faults, regional studies, Nevada and California: U. S. Geological Survey, Open-File Report 95-0599.

dePolo, C. M., and A. R. Ramelli, 1996, Quaternary and suspected Quaternary faults in Nevada south of 37° N. latitude: presented at the Seismic Hazards in the Las Vegas Region conference, Nov. 14-15, Las Vegas.

Dokka, R. K., and C. J. Travis, 1990, Role of the eastern California shear zone in accommodating Pacific-North American plate motion: Geophysical Research Letters, v. 17, p. 1323-1326.

Donovan, Diane E., 1991, Neotectonics of the southern Amargosa Desert, Nye County, Nevada and Inyo County, California: University of Nevada, Reno M.S. thesis 2755, 151 pp.

Hillhouse, J. W., 1987, Late Tertiary and Quaternary geology of the Tecopa basin, southeastern California: U.S. Geological Survey Miscellaneous Investigations Map I-1728, scale 1:48,000, 1 sheet, 16 pp. text.

Hoffard, Joanne L., 1991, Quaternary tectonics and basin history of Pahrump and Stewart Valleys, Nevada and California: University of Nevada, Reno M.S. thesis 2747, 138 pp.

Louie, J. N., R. W. Clayton, and R. J. Le Bras, 1988, Three-dimensional imaging of steeply dipping structure near the San Andreas fault, Parkfield, California: Geophysics, v. 53, p. 176-185.

Lumley, D. E., J. F. Claerbout, and D. Bevc, 1994, Anti-aliased Kirchhoff 3-d migration: Society of Exploration Geophysicists Annual International Meeting, Los Angeles, October, Expanded Abstracts, p. 1282-1285.

MIT Field Geophysics Course, 1985, A Geophysical Study of Mesquite Valley, Nevada-California Border: Journal of Geophysical Research, v. 90, p. 8685-8690.

Morrison, R. B., 1991, Quaternary stratigraphic, hydrologic, and climatic history of the Great Basin, with emphasis on Lakes Lahontan, Bonneville, and Tecopa: in Morrison, R. B., ed., Quaternary Non-Glacial Geology, Conterminous U.S., Boulder, Colorado, Geological Society of America, Geology of North America, v. K-2, p. 283-320.

Piety, L. A., 1996, Compilation of known or suspected Quaternary faults within 100 km of Yucca Mountain: U. S. Geological Survey, Open-File Report 94-0112, 1:250,000.

Quade, J., M. D. Mifflin, W. L. Pratt, W. McCoy, and L. Burckle, 1995, Fossil spring deposits in the southern Great Basin and their implications for changes in water-table levels near Yucca Mountain, Nevada, during Quaternary time: Geological Society of America Bulletin, v. 107, p. 213-230.

Sawyer, T. L., R. E. Klinger, C. M. dePolo, and M. C. Reheis, 1996, Death Valley fault system: significant ground motion sources for southern Nevada: presented at the Seismic Hazards in the Las Vegas Region conference, Nov. 14-15, Las Vegas.

Schweickert, R. A., and M. M. Lahren, 1994, Amargosa fault system near Yucca Mountain, Nevada: Abstracts with Programs, Geological Society of America, v. 26, no. 7, p. 250.

Shields, G., K. Allander, R. Brigham, R. Crosbie, L. Trimble, M. Sleeman, R. Tucker, H. Zhan, and J. N. Louie, 1996, Geophysical surveys of an active fault: results from southern Pahrump Valley, California-Nevada border: submitted to Bulletin of the Seismological Society of America, 1 June.

Slemmons, D. B., 1996, Seismotectonic setting for the Las Vegas basin, Nevada: presented at the Seismic Hazards in the Las Vegas Region conference, Nov. 14-15, Las Vegas.

Smith, K., D. dePolo, S. Gross, D. Von Seggern, G. Biasi, J. G. Anderson, J. N. Brune, and C. dePolo, 1996, Historical earthquakes and recorded seismicity of the southern Great Basin in the vicinity of Las Vegas, Nevada: presented at the Seismic Hazards in the Las Vegas Region conference, Nov. 14-15, Las Vegas.

Su, F., and J. G. Anderson, 1996, Basin effects on strong motion in Las Vegas: presented at the Seismic Hazards in the Las Vegas Region conference, Nov. 14-15, Las Vegas.

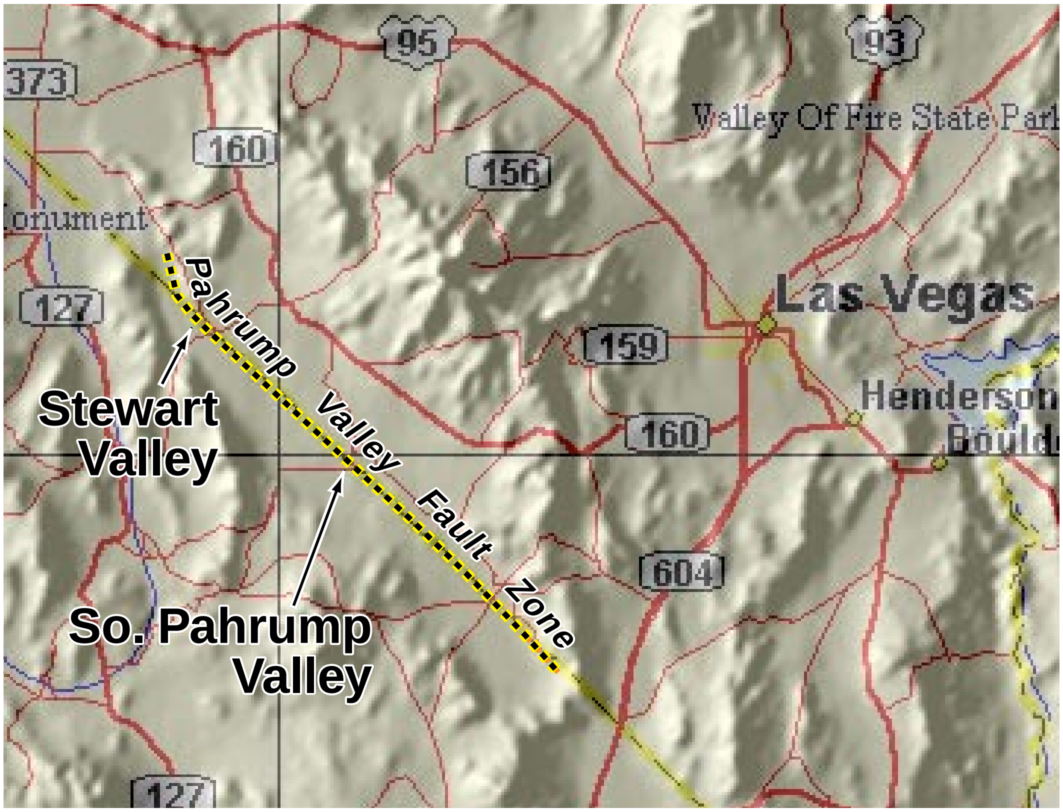

Figure 1: map showing our two geophysical study areas along the Pahrump Valley fault zone (PVFZ) 50 km west of Las Vegas.

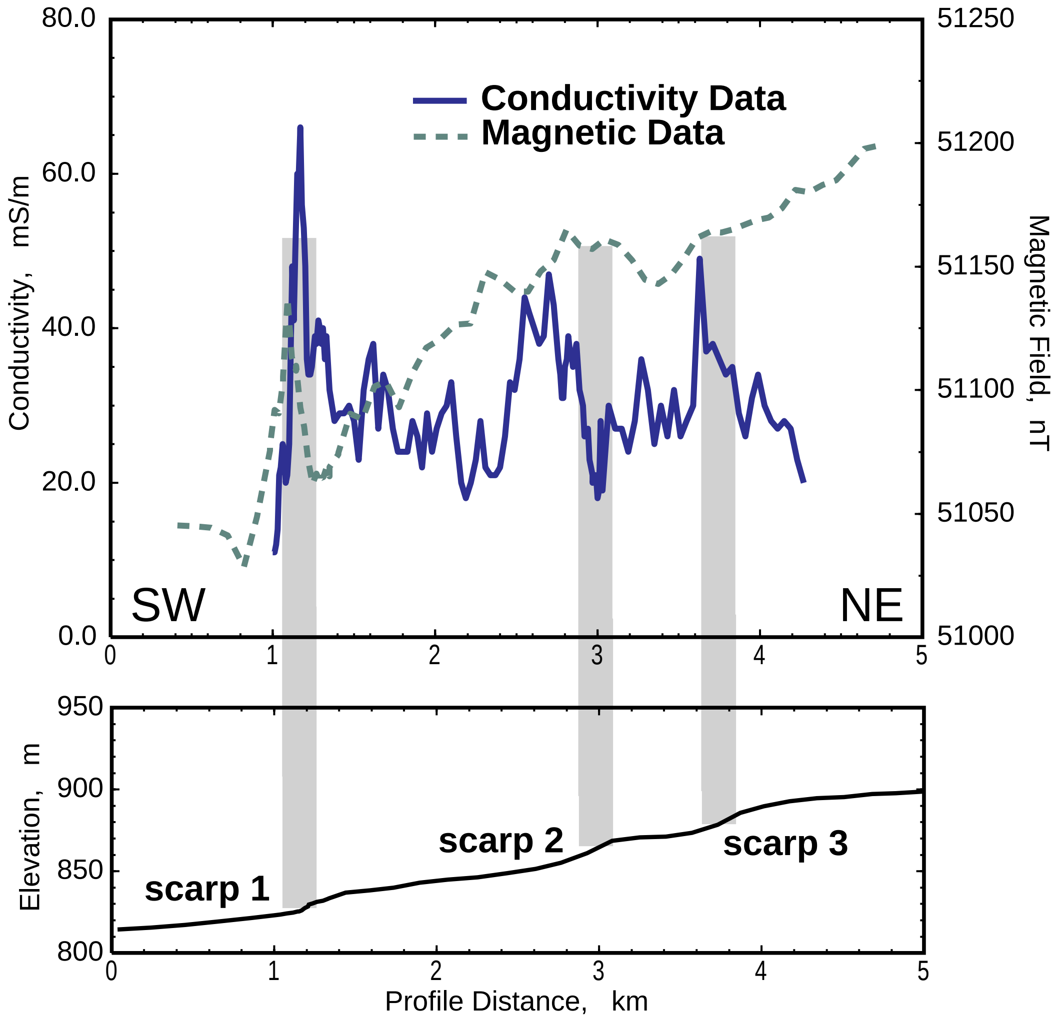

Figure 2: elevation profile (bottom) along the Old Spanish Trail Highway, showing the three scarps, with the state border at 700 m distance. Above are the results of shallow (< 3 m) ground conductivity measurements (solid line) made with a Geonics EM-31 instrument along the road, together with total-field magnetometer measurements (dashed line). The magnetic survey extended completely across Pahrump Valley; only the section crossing the fault zone is shown here. The overall increase in magnetic field toward the east is due to a large regional magnetic anomaly centered at the Spring Mountains.

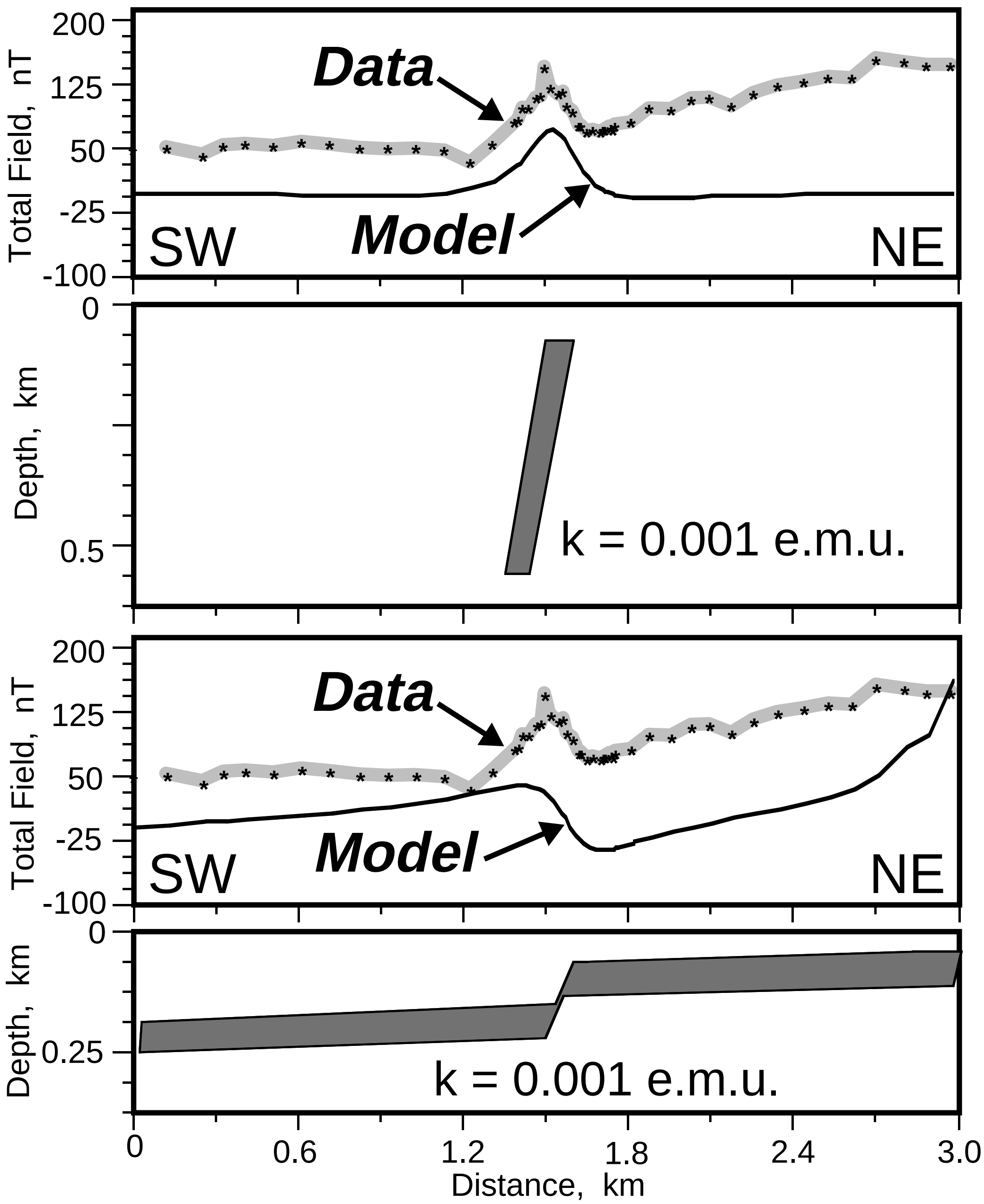

Figure 3: trial magnetic models for the southern Pahrump Valley scarp 1. This section shows just the scarp 1 anomaly seen on the left side of fig. 2. Edge effects of the faulted near-horizontal-layer model create an asymmetry that matches the data poorly, while the steeply-dipping fault-zone-inclusion model creates a more symmetric fit. Vertical exaggeration of cross sections is 1.8 times.

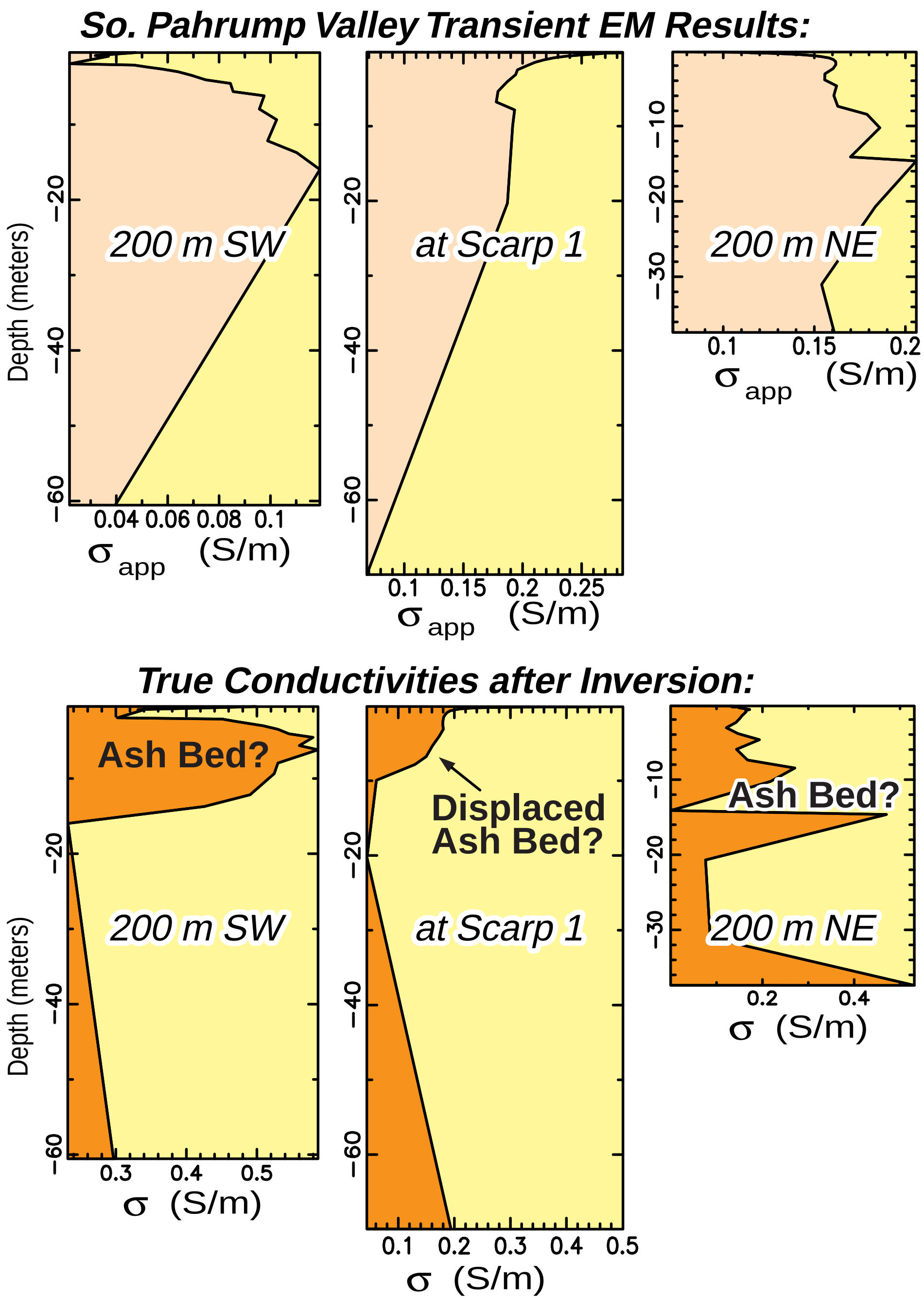

Figure 4: analysis of the three TEM soundings in southern Pahrump Valley at three locations: at scarp 1; and 200 m southwest and 200 m northeast of scarp 1. The upper columns depict raw apparent conductivity measurements plotted against the transient time-depth. The lower columns plot interval conductivities against true depth.

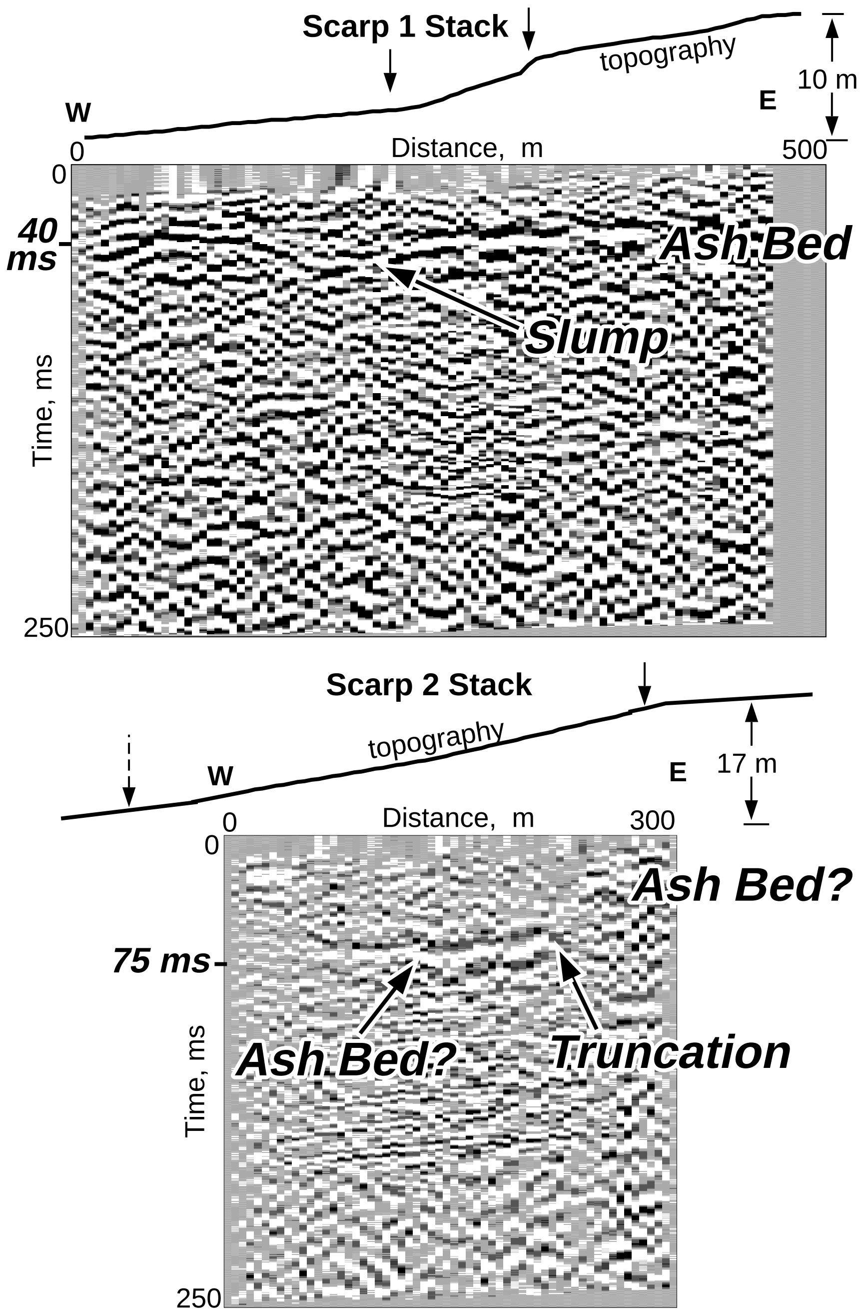

Figure 5: 2-d high-resolution seismic stacked sections across PVFZ scarps 1 and 2 in southern Pahrump Valley. Note that the vertical scale bars apply only to the scarp profiles. The 40 ms two-way travel time implies a depth of the reflective bed of about 30 m, and the 75 ms time about twice that depth, yielding an approximately 1.3 times vertical exaggeration of the sections.

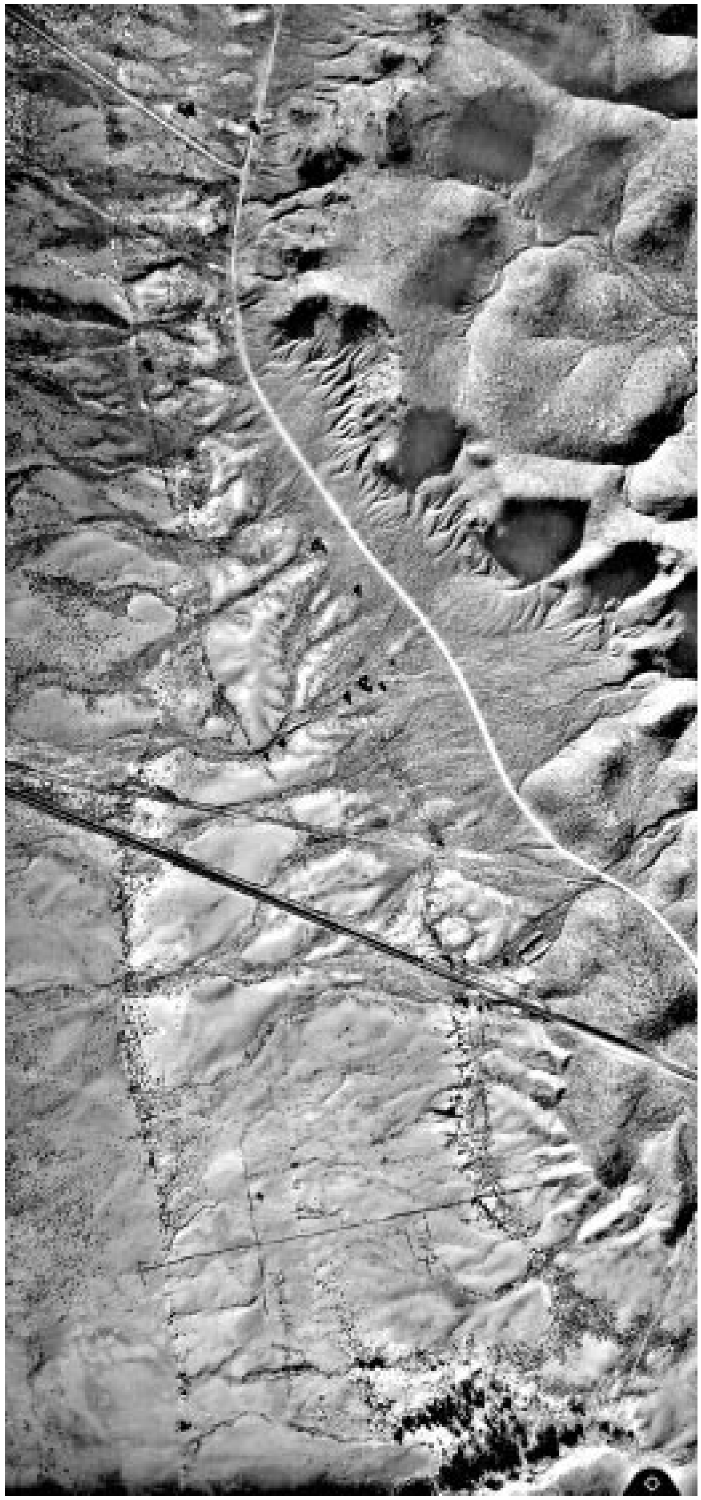

Figure 6: enhanced low-sun-angle air photo of PVFZ traces in southern Stewart Valley. North is toward the upper right. Our study area is located along the fault about midway between the two east-west roads.

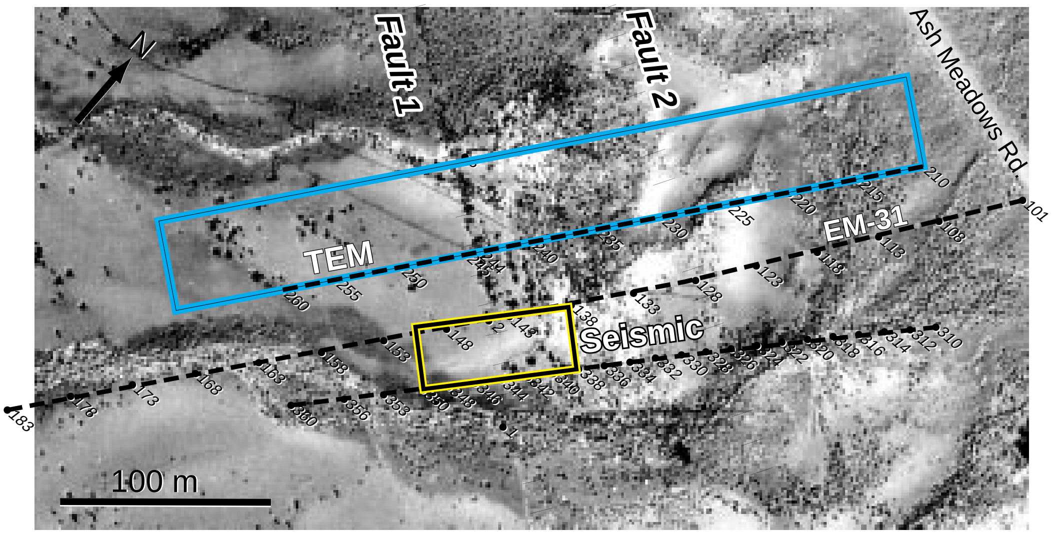

Figure 7: section of air photo in fig. 6 showing the locations of our geophysical surveys in Stewart Valley. Station EM344, on the south side of our 3-d seismic reflection survey area, is on the most continuous vegetation lineament and in the middle of the gravity line, and on one of three lines where we took Geonics EM-31 shallow ground conductivity and magnetic measurements. The northern of the three lines was the basis for our layout of eight adjacent 40 m square TEM transmitter loops. The main trace of the PVFZ at the most continuous vegetation lineament is the hatched line at left (fault 1); while the hatched line to the right denotes a topographic scarp and second trace cutting the spring mounds, or possibly a Pluvial lake terrace (fault 2).

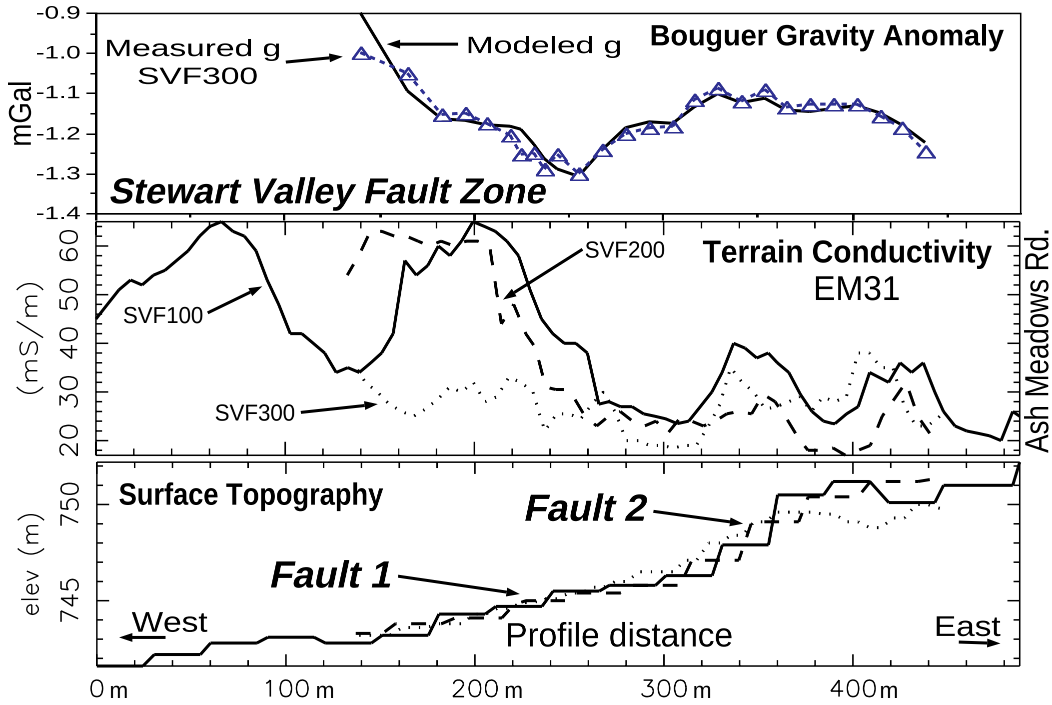

Figure 8: gravity, EM-31 shallow conductivity, and elevation profiles across faults 1 and 2 on the PVFZ in Stewart Valley.

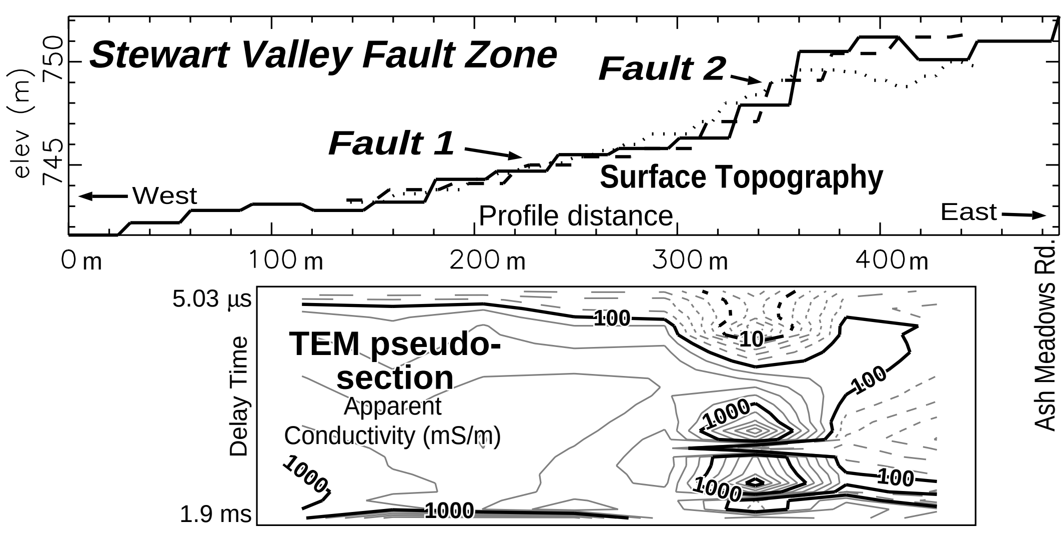

Figure 9: elevation profiles and TEM pseudosection across the PVFZ in Stewart Valley.

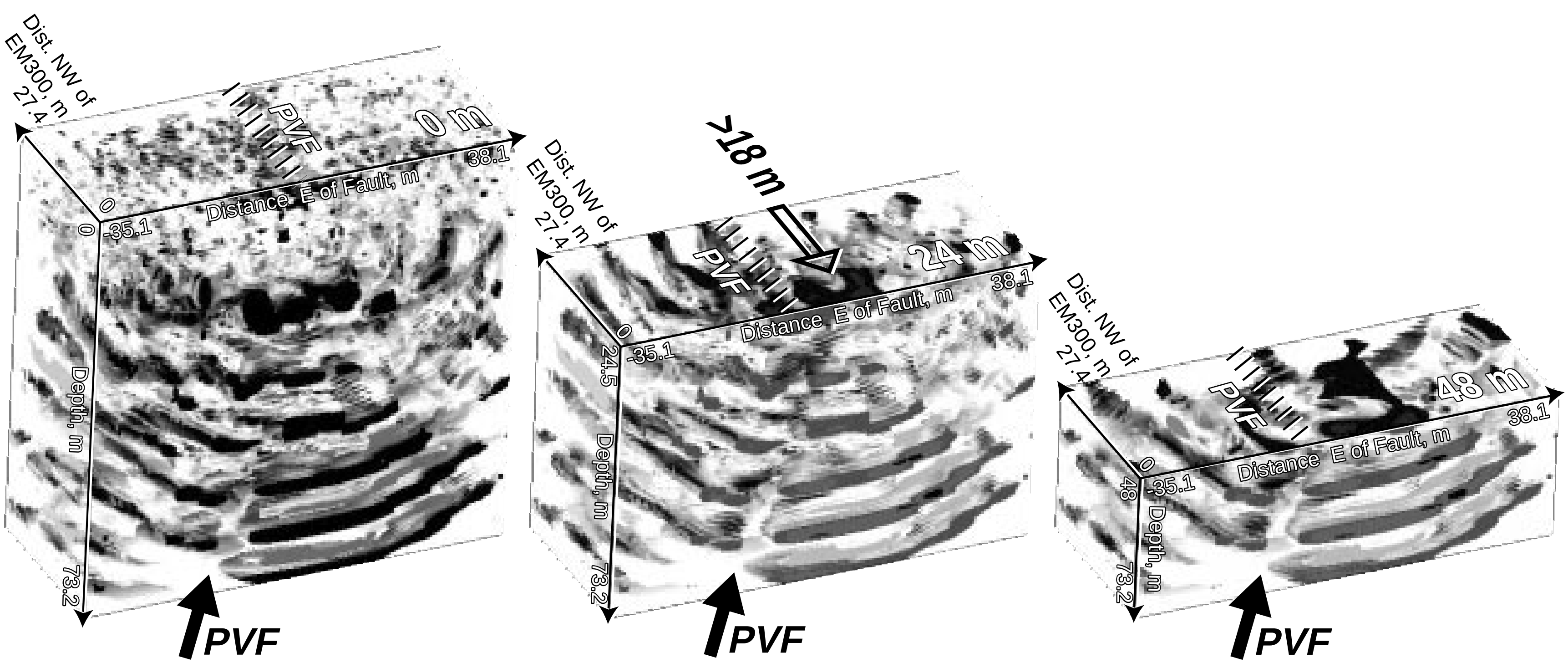

Figure 10: 3-d seismic image volume 73 m wide, 27 m thick, and 73 m deep across PVFZ fault 1 in Stewart Valley (fig. 7), rendered to emphasize the positive reflectivities of greatest amplitude as darkly shaded, opaque 3-d objects. Near-zero reflectivities are rendered transparent. The whole volume is at left, and the two at center and right show depth slices at 24 and 48 m, respectively. The upward curving of the reflectors at the edges is a migration artifact; note the gaps in the layers where fault 1 passes through (PVF).